



Sitbon, G., Chantrell, R., & Schwarzacher, W. (2020). The effects of anisotropy on solvent-suspended 'superparamagnetic' nanoparticles: magnetization step on melting. *Journal of Magnetism and Magnetic Materials*, 503, [166486]. <https://doi.org/10.1016/j.jmmm.2020.166486>

Peer reviewed version

License (if available):  
CC BY-NC-ND

Link to published version (if available):  
[10.1016/j.jmmm.2020.166486](https://doi.org/10.1016/j.jmmm.2020.166486)

[Link to publication record in Explore Bristol Research](#)  
PDF-document

This is the author accepted manuscript (AAM). The final published version (version of record) is available online via Elsevier at <https://www.sciencedirect.com/science/article/pii/S0304885319329130>. Please refer to any applicable terms of use of the publisher.

## University of Bristol - Explore Bristol Research

### General rights

This document is made available in accordance with publisher policies. Please cite only the published version using the reference above. Full terms of use are available:  
<http://www.bristol.ac.uk/red/research-policy/pure/user-guides/ebr-terms/>

# The effects of anisotropy on solvent-suspended 'superparamagnetic' nanoparticles: magnetization step on melting

G. Sitbon<sup>1</sup>, W. Schwarzacher<sup>1\*</sup> and RW Chantrell<sup>2</sup>

<sup>1</sup>H H Wills Physics Laboratory, University of Bristol, Tyndall Avenue, Bristol BS8 1TL

<sup>2</sup> Physics Department, University of York, York, YO10 5DD, UK

\*w.schwarzacher@bristol.ac.uk

## Abstract

The magnetic anisotropy of single-domain magnetic nanoparticles can influence their behaviour significantly even at temperatures above the blocking temperature as conventionally defined. We compare the magnetic properties of such nanoparticles that are free to rotate, and the same nanoparticles with random but fixed orientations. When free to rotate, the particles show Langevin behaviour as expected, but when the orientations are fixed, their magnetic anisotropy causes deviations from this behaviour. These deviations may be observed directly in the  $M - H$  curves. They also cause a step in the  $M - T$  curve measured for a zero-field cooled sample of nanoparticles suspended in a solvent at the solvent's melting point. The step occurs because magnetic anisotropy causes  $M$  for particles with random but fixed orientation to be lower than for the same particles that are free to rotate when the solvent melts. The size of the step reaches a maximum at a finite applied field. This phenomenon is important because it can be used to determine the fraction of magnetic nanoparticles that are immobilized, for example by adsorption to ice in a freeze-concentrated solution.

## Keywords:

Fine particle magnetism; superparamagnetism; ferrofluid; Brownian motion; magnetic anisotropy.

## Introduction

The magnetic properties of single-domain magnetic nanoparticles have been widely studied, motivated by their applications as magnetic recording media [1], ferrofluids [2] and in biomedicine [3] as well as by their intrinsic interest. At sufficiently low temperatures and in the absence of an applied field, magnetic anisotropy will keep the magnetization direction of each particle fixed relative to its orientation. As the temperature increases, the thermal energy becomes comparable to the magnetic anisotropy energy and the timescale for magnetic fluctuations decreases. At sufficiently high temperatures, although the nanoparticle remains magnetically ordered, its magnetic moment fluctuates like that of a paramagnet and the particle's behaviour is described as 'superparamagnetic' [4]. The magnetization  $M$  obeys the Langevin equation

$$\frac{M}{M_s} = \coth \alpha - \frac{1}{\alpha} \quad (1)$$

where  $M_s$  is the saturation magnetization and  $\alpha = \frac{\mu H}{kT}$ . In the expression for  $\alpha$ ,  $\mu$  is the magnitude of the particle magnetic dipole moment,  $H$  is the applied magnetic field,  $k$  is Boltzmann's constant and  $T$  is the temperature. Conventionally, the superparamagnetic blocking temperature is defined by  $T_B = \frac{KV}{25k}$ , where  $K$  is the magnetic anisotropy energy per unit volume  $V$ . Above  $T_B$  fluctuations are observed on the timescale of a typical magnetization measurement ( $\tau_m = 100$  sec) and consequently the  $M$ - $H$  curve is hysteresis-free. However, this does not mean that the magnetic anisotropy can be ignored.

Here we show how the magnetic anisotropy above  $T_B$  enables detection of the onset of free rotation of a magnetic nanoparticle i.e. the point at which magnetic relaxation occurs by Brownian rotation in addition to the Néel-Brown mechanism [5]. We consider the example of nanoparticles that are immobilized in a solid matrix that become free to rotate at the melting point of the matrix [6]. Through experimental data and simulation, we show that for zero field-cooled samples a step-like increase is observed in  $M(T)$  measured on heating at constant  $H$  when the melting point is reached. The size of the step depends on the magnitude of  $H$ ,  $T$  and the magnetic anisotropy energy  $KV$ . The step vanishes as  $H \rightarrow 0$ .

The phenomenon we describe has a number of useful applications. Beyond the simple example of a matrix that melts abruptly as discussed above, where it can be used in melting point determinations, it can also be used to probe glass transitions. In the case of a glass transition, rather than an abrupt transition from a solid to a liquid, there is a continuous decrease in the viscosity of the matrix. A step is still observed [7], this time at the temperature  $T_R$  at which the timescale for Brownian rotation reaches  $\tau_m$ . The value of  $T_R$  contains useful information about the system, as it is proportional to  $\eta a^3$ , where  $\eta$  is the viscosity of the matrix at  $T = T_R$ , and  $a$  is the nanoparticle hydrodynamic radius. In addition to the temperature of the step, its magnitude can be of interest, because it depends on the number of nanoparticles that become free to rotate at  $T_R$ . Hence the step height measured for a freeze-concentrated aqueous solution of nanoparticles that also contains pure ice can be used to detect nanoparticles immobilized e.g. by adsorption to ice, because the immobilized nanoparticles unlike those in the freeze-concentrated phase, do not contribute to the step [8]. Steps are also seen in  $M(T)$  measurements of field-cooled samples [7]. Although the observed step size can be greater for field-cooled samples, working with zero field-cooled samples has the advantage that any field-induced aggregation of the magnetic nanoparticles while the solvent is still liquid during cooling is avoided.

## Results and discussion

We dissolved samples of commercially available  $\text{Fe}_3\text{O}_4$  nanoparticles (15 nm nominal diameter, < 5% size distribution, coated with oleic acid, supplied by Ocean NanoTech) in a series of alkane solvents with increasing melting point: hexane (melting point  $\approx 178$  K), octane (melting point  $\approx 216$  K,) and decane (melting point  $\approx 243$  K). In each case, the nanoparticle concentration was  $\sim 6 \times 10^{-8}$  M. Each sample was cooled in zero applied field to well below the solvent melting point, then its magnetization measured as the temperature was raised at a rate of  $\sim 1$  K/min in an applied field  $H = 100$  Oe using a SQUID magnetometer (Quantum Design MPMS). The results are shown in Figure 1. Each  $M - T$  curve exhibits a clear step, and the temperature at which it is observed increases with the molecular weight of the solvent. The quoted melting points (indicated by arrows in the figure) correspond closely to the temperatures at which the steps commence. For comparison, Figure 2 shows data for the same nanoparticles with water as the solvent. To make the nanoparticles water-soluble, we carried out a ligand exchange using 3,4-dihydroxybenzoic acid (DHBA) to replace oleic acid with hydrophilic ligands. For this experiment the temperature was raised at a rate of  $\sim 3$  K/min. Figure 2 shows a clear increase at the melting point of ice, confirming that this phenomenon is not restricted to alkanes. The data also shows the broad peak in the zero field-cooled  $M - T$  data characteristic of a sample of superparamagnetic nanoparticles that relax by the Néel-Brown mechanism. The peak is caused by nanoparticles reaching  $T_B$  and is broad because the particles are not ideally monodisperse and can interact via dipolar interactions.

To understand the origin of the steps, consider a system of nanoparticles in a fluid environment. Since the particle is free to rotate, the direction of its magnetic moment is unconstrained, and this is true even if the particle's orientation and magnetization direction are coupled by magnetic anisotropy. Hence the magnetization is independent of the magnetic anisotropy and is given by the Langevin function. Rather than alter the magnetization, the effect of the magnetic anisotropy is to modify the probability that the particle has a given orientation, giving rise to a preferential easy axis orientation [9, 10].

The situation of a nanoparticle in a solid environment is quite different. Since any magnetic anisotropy present will couple the direction of the particle's magnetic moment to its orientation, and the latter is constrained by being in a solid, the direction of the particle's magnetic moment is also constrained. Hence the magnetization is no longer simply given by the Langevin function [11-13]. Figure 3 shows how the simulated magnetization of a system of monodisperse, non-interacting particles in a solid environment depends on the applied field (parametrized as  $\alpha = \frac{\mu H}{kT}$ ) and the magnetic anisotropy (parametrized as  $\beta = \frac{KV}{kT}$ ). The simulations use a kinetic Monte-Carlo model that allows thermally activated transitions over energy barriers provided by the local anisotropy with a probability determined by the Arrhenius-Néel law [14]. We assume the particles have fixed but random easy axis directions, as appropriate for a sample cooled below the solvent melting point in zero applied field.

When a sample like those of Figure 1 passes through the solvent melting point on warming in an applied field  $H$ ,  $M$  changes from lying on one of the family of curves shown in Figure 3 to being given by the Langevin function. However, the Langevin function is simply the curve in Figure 3 corresponding to  $\beta = 0$ . Hence, when the sample passes through the solvent melting point,  $M$  changes from  $M(\alpha, \beta)$  to  $M(\alpha, 0)$ . From Figure 3, it is clear that  $\Delta M = M(\alpha, 0) - M(\alpha, \beta)$  is positive, so there is a positive step in  $M$ , as seen in Figure 1. Furthermore, for a given  $\alpha$ , the greater the magnetic anisotropy  $K$ , the greater  $\beta$ , the lower  $M(\alpha, \beta)$  and hence the greater the step height  $\Delta M$ .

Note that the step height also depends on  $\alpha$ . As  $\alpha$  tends to zero, the separation of the curves in Figure 3 and hence  $\Delta M$  also tend to zero. This disappearance of the magnetization step for small  $\alpha$  is expected because it was shown in reference [15] that when  $H$  tends to zero for a system of nanoparticles in a solid environment,  $\frac{M}{M_s}$  tends to  $\chi H$ , where

$$\chi = \frac{\mu}{kT} \left( \langle \cos^2 \theta \rangle + \frac{1}{2} (1 - 3 \langle \cos^2 \theta \rangle) f(\beta) \right) \quad (2).$$

In this equation,  $\theta$  is the angle between the easy axis and the applied field and  $f(\beta)$  is a function of  $\beta$  defined in [15]. Since  $\langle \cos^2 \theta \rangle = \frac{1}{3}$  for a random distribution of easy axis directions, as in Figure 3,  $\chi = \frac{\mu}{3kT}$ , and is independent of  $\beta$ . This also means that the initial susceptibility of a system of nanoparticles in a solid environment with random easy axis directions is the same as it would be for those nanoparticles in a fluid environment. As  $\alpha$  tends to infinity, the separation of the curves in Figure 1 and therefore the step height  $\Delta M$  will again tend to zero. This is because for all  $\beta$ ,  $M$  approaches  $M_s$ . Hence  $\Delta M$  must go through a maximum as a function of  $\alpha$ . This means that there is an optimum range of values for the field  $H$  applied when warming a zero field-cooled sample through the solvent melting point in order to see a significant step in the  $M - T$  curve.

Figure 4 illustrates this point by showing simulated  $M - T$  curves for a system of ferrite particles ( $M_s = 400 \text{ emu cm}^{-3}$ ) of diameter 12.5 nm and magnetic anisotropy energy  $K = 2.4 \times 10^5 \text{ erg cm}^{-3}$  warmed in various applied fields  $H$  following cooling in zero field. A field dependent step at the assumed melting point  $T = 200 \text{ K}$  is seen, the height of which depends on  $H$ . The jump in  $M$  at lower temperatures is due to the transition from stable ferromagnetic behaviour to superparamagnetic behaviour. The temperature at which this transition occurs depends on the applied field  $H$ . The transition is very sharp due to the monodispersity of the system.

To compare with these simulations, we also measured  $M - T$  curves for a sample of the same 15 nm commercially available  $\text{Fe}_3\text{O}_4$  nanoparticles in decane warmed at  $\sim 0.5 \text{ K/min}$  in various applied fields following cooling from above to well below the solvent melting point in zero field. The results are shown in Figure 5. From the figure, the step height  $\Delta M$  initially increases with  $H$ , consistent with the predictions of Figure 4. For  $H = 500 \text{ Oe}$ , however, the step height is less than for  $H = 200 \text{ Oe}$ , which confirms our conclusion above that  $\Delta M$  must go through a maximum as a function of  $\alpha$ , and hence of  $H$ .

Figure 6 shows  $M - H$  curves for 15 nm  $\text{Fe}_3\text{O}_4$  nanoparticles in decane measured at  $T = 220 \text{ K}$  and  $T = 260 \text{ K}$ , i.e. below and above the melting point of the solvent. The data is plotted as a function of  $H/T$ . From Figure 3, we expect that when the data is plotted in this way, the curve measured below the melting point will saturate more slowly than that measured above, due to the influence of anisotropy below the melting point ( $\beta > 0$ ). Though the data is noisy, this does indeed appear to be the case. However, the effect of melting is seen much more clearly in the  $M - T$  curves measured at fixed applied field than in the  $M - H$  curves (compare Figures 5 and 6). Hence we believe that the former are more useful for applications such as probing freeze concentration.

## Conclusions

Since the  $M - H$  curve for magnetic nanoparticles that are free to rotate is given by the Langevin function, while the  $M - H$  curve for the same nanoparticles when their orientations are fixed is influenced by their magnetic anisotropy, the magnetization of an assembly of nanoparticles suspended in a solvent can change at the solvent melting point. In this paper we focussed on nanoparticles cooled in zero field and warmed in an applied field  $H$ , since this situation is relevant to

e.g. studies of freeze concentration [1], and showed that in the  $M - T$  curve a step is expected at the solvent melting point. The step size goes through a maximum, as the difference between the  $M - H$  curves for fixed, randomly oriented nanoparticles and freely-rotating nanoparticles tends to zero for  $H \rightarrow 0$  and  $H \rightarrow \infty$ . Experimental data confirmed the presence of the step at the expected value of  $T$  for three different alkane solvents, and that the step height varies with  $H$  for decane.

### **Acknowledgements**

This work was funded by a Leverhulme Trust Research Project Grant, no. RPG-2014-180.

## References

- [1] E.P. Wohlfarth, Review of Problem of Fine-Particle Interactions with Special Reference to Magnetic Recording, *J. Appl. Phys.*, 35 (1964) 783-790.
- [2] R.E. Rosensweig, Magnetic Fluids, *Ann. Rev. Fluid Mech.*, 19 (1987) 437-463.
- [3] Q.A. Pankhurst, N.T.K. Thanh, S.K. Jones, J. Dobson, Progress in applications of magnetic nanoparticles in biomedicine, *J. Phys. D - Appl. Phys.*, 42 (2009).
- [4] B.D. Cullity, C.D. Graham, *Introduction to Magnetic Materials*, Second ed., John Wiley & Sons, Inc., Hoboken, New Jersey, U.S.A., 2009.
- [5] J.L. Zhang, C. Boyd, W.L. Luo, Two mechanisms and a scaling relation for dynamics in ferrofluids, *Phys. Rev. Lett.*, 77 (1996) 390-393.
- [6] T.L. Wen, W.K. Liang, K.M. Krishnan, Coupling of blocking and melting in cobalt ferrofluids, *J. Appl. Phys.*, 107 (2010) 09B501.
- [7] J.C. Eloi, M. Okuda, S.E.W. Jones, W. Schwarzacher, Protein Brownian Rotation at the Glass Transition Temperature of a Freeze-Concentrated Buffer Probed by Superparamagnetic Nanoparticles, *Biophys. J.*, 104 (2013) 2681-2685.
- [8] E.F. Chagas, S.C. Carreira, W. Schwarzacher, Using magnetic nanoparticles to probe protein damage in ferritin caused by freeze concentration, *AIP Adv.*, 5 (2015) 117201.
- [9] R.W. Chantrell, B.K. Tanner, S.R. Hoon, Determination of the Magnetic-Anisotropy of Ferrofluids from Torque Magnetometry Data, *J. Magn. Magn. Mater.*, 38 (1983) 83-92.
- [10] C. Johansson, M. Hanson, P. Lundqvist, Field-induced anisotropy in a magnetic liquid, *J. Magn. Magn. Mater.*, 157/158 (1996) 599-600.
- [11] Y.L. Raikher, The Magnetization Curve of a Textured Ferrofluid, *J. Magn. Magn. Mater.*, 39 (1983) 11-13.
- [12] U. Hartmann, H.H. Mende, Anisotropic Superparamagnetic Behavior in Textured Ferrofluid Systems, *Philos Mag B*, 52 (1985) 889-897.
- [13] H.D. Williams, K. Ogrady, M. Elhilo, Superparamagnetism in Fine Particle Dispersions, *J. Magn. Magn. Mater.*, 122 (1993) 129-133.
- [14] R.W. Chantrell, N. Walmsley, J. Gore, M. Maylin, Calculations of the susceptibility of interacting superparamagnetic particles, *Phys. Rev. B*, 63 (2001) 24410.
- [15] R.W. Chantrell, N.Y. Ayoub, J. Popplewell, The Low Field Susceptibility of a Textured Superparamagnetic System, *J. Magn. Magn. Mater.*, 53 (1985) 199-207.

Figures:

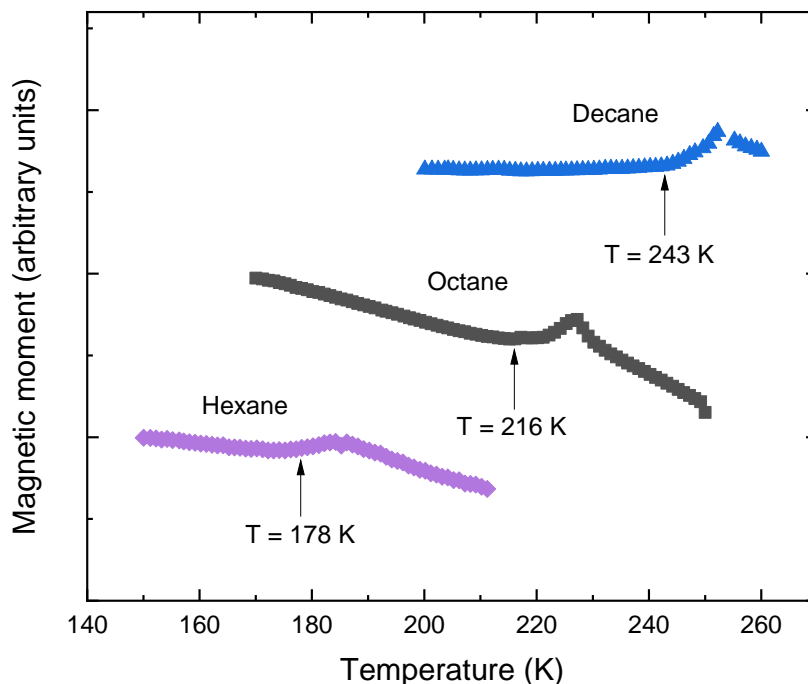


**Figure 1:**  $M - T$  curves measured for commercially available Fe<sub>3</sub>O<sub>4</sub> nanoparticles of nominal diameter 15 nm dissolved in hexane, octane and decane. Samples were cooled in zero applied field to well below the solvent melting point, then their magnetizations measured as the temperature was raised in an applied field  $H = 100 \text{ Oe}$ . Curves have been offset vertically for clarity. A Quantum Design MPMS XL system working in reciprocating sample option scan mode was used for these measurements.

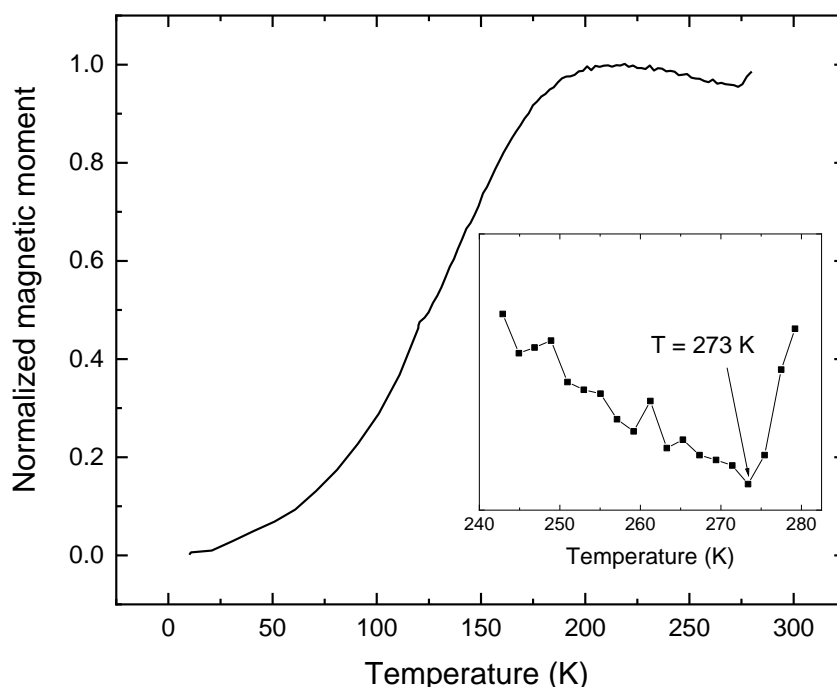


**Figure 2:**  $M - T$  curve measured for commercially available Fe<sub>3</sub>O<sub>4</sub> nanoparticles of nominal diameter 15 nm dissolved in water, following ligand exchange. The sample was cooled in zero applied field, then the magnetization measured as the temperature was raised in an applied field  $H = 50 \text{ Oe}$ . The inset shows the data close to  $T = 273 \text{ K}$  in greater detail. A Quantum Design MPMS 3 was used for these measurements.



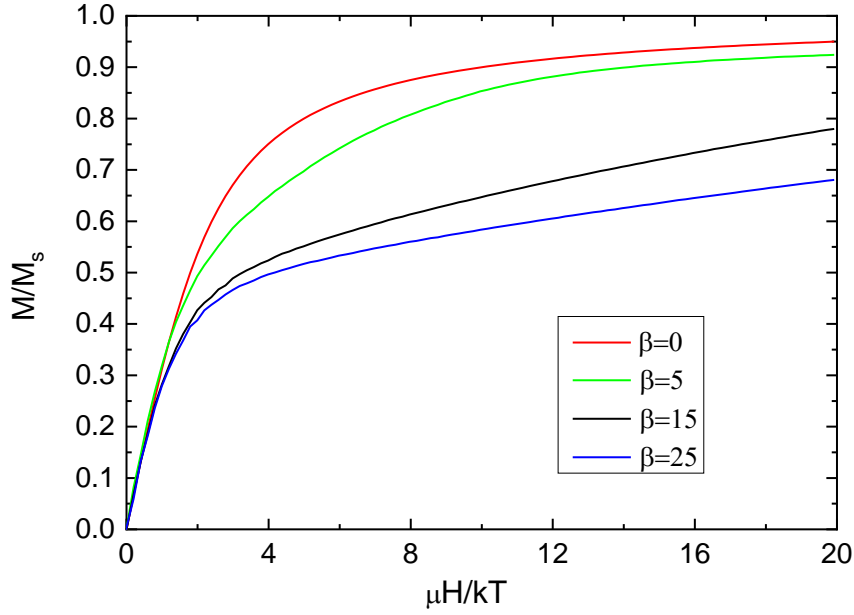


**Figure 3:** Magnetization  $M$  normalized to the saturation magnetization  $M_s$ , simulated for a system of monodisperse, randomly oriented, non-interacting particles in a solid environment. The different colours correspond to different values of the parametrized magnetic anisotropy  $\beta = \frac{KV}{kT}$  (see text).

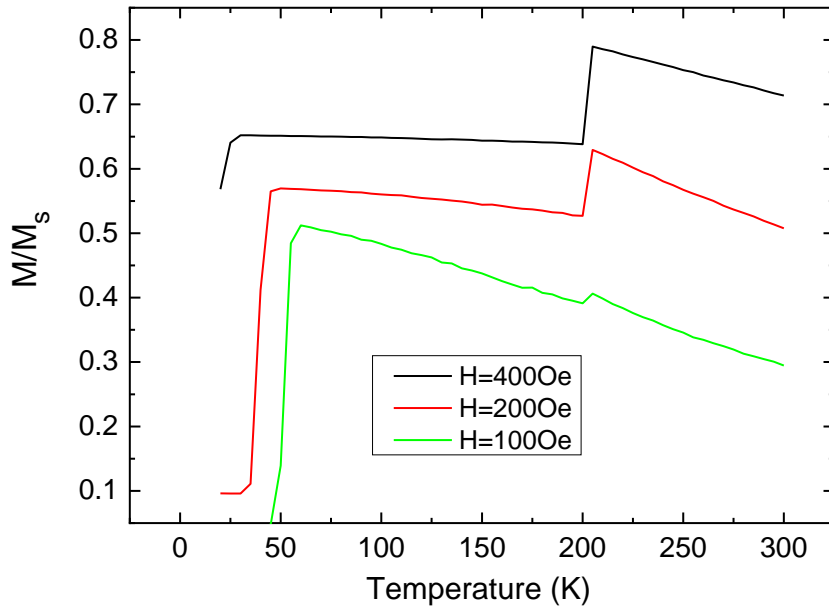


**Figure 4:** Normalized magnetization as a function of temperature  $T$ , simulated for a system of ferrite particles ( $M_s = 400 \text{ emu cm}^{-3}$ ) of diameter 12.5 nm and magnetic anisotropy energy  $K = 2.4 \times 10^5 \text{ erg cm}^{-3}$  suspended in a solvent having melting point  $T = 200 \text{ K}$ . The particles are cooled in zero field before warming through the solvent melting point in applied field  $H$ .

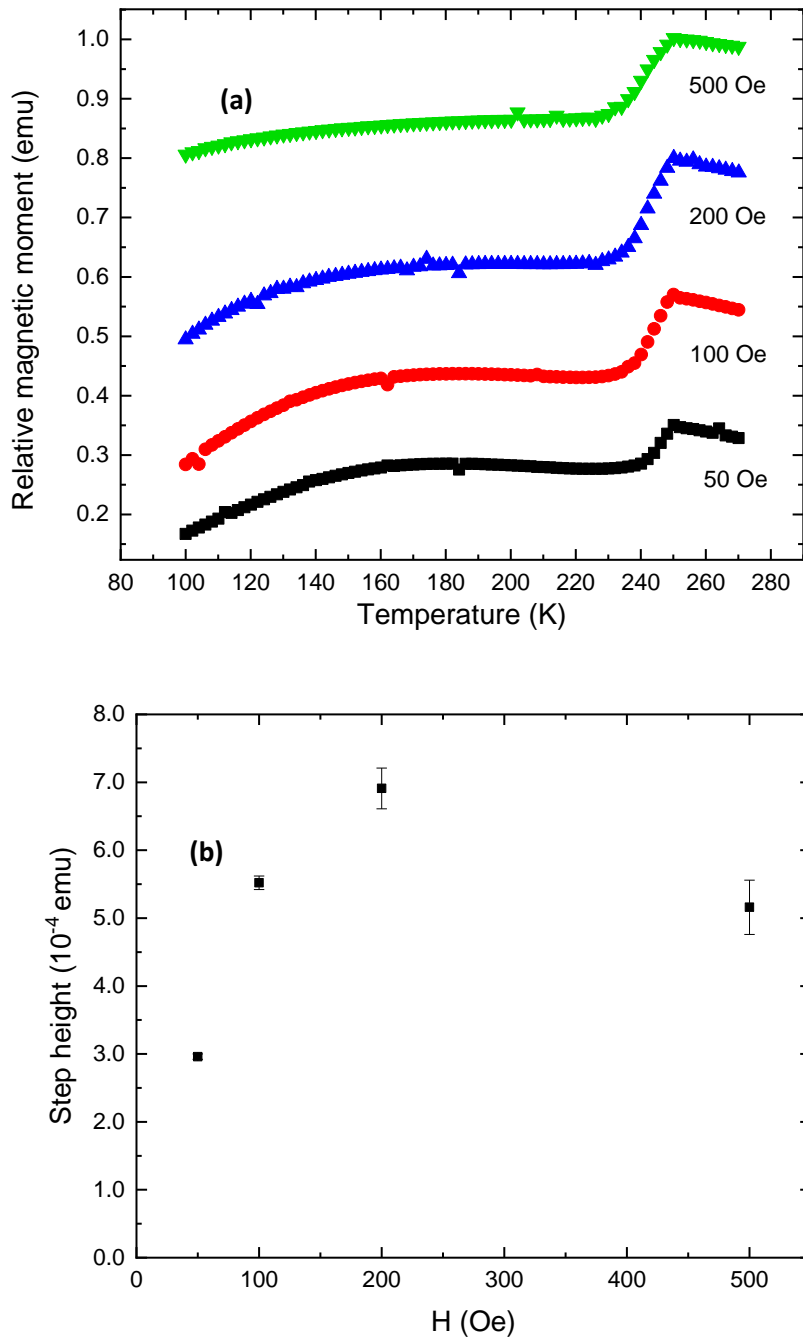


**Figure 5:** (a)  $M - T$  curves measured for commercially available  $\text{Fe}_3\text{O}_4$  nanoparticles of nominal diameter 15 nm dissolved in decane. Samples were cooled in zero applied field to well below the solvent melting point, then their magnetizations measured as the temperature was raised in different applied fields  $H$  indicated on the Figure. A Quantum Design MPMS XL system working in DC scan mode was used for these measurements. Data are normalized to the maximum measured moment to emphasize relative changes on varying the applied field. (b) Step height ( $\Delta M$ ) as a function of

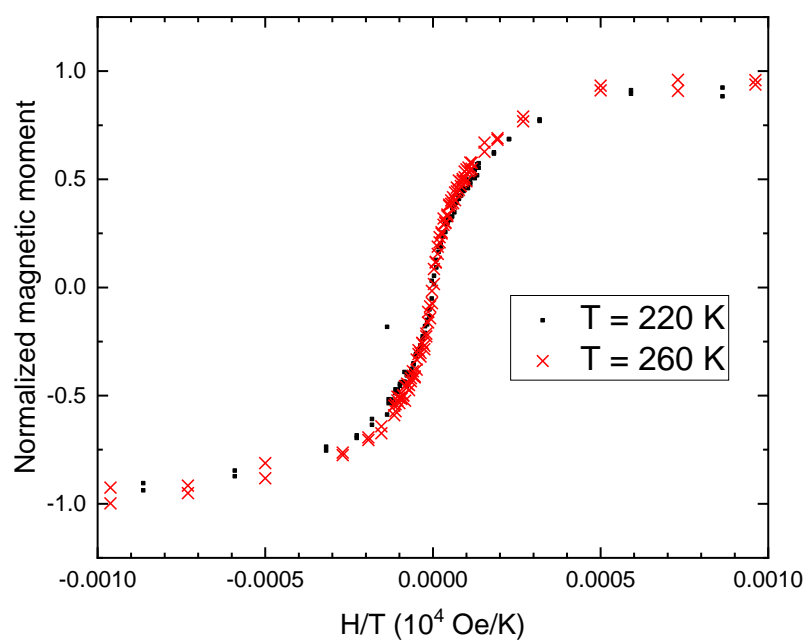


**Figure 6:** Normalized  $M$  as a function of  $H/T$  for 15 nm  $\text{Fe}_3\text{O}_4$  nanoparticles in decane measured at  $T = 220$  K and  $T = 260$  K. The same diamagnetic background was subtracted from each set of data, and the same normalization factor applied to each. A Quantum Design MPMS XL system working in DC scan mode was used for these measurements.